# Enzyme Selection, Optimization, and Production toward Biodegradation of Post-Consumer Poly(ethylene terephthalate) at Scale

Ya-Hue Valerie Soong [a], Umer Abid [a], Allen C. Chang [b], Christian Ayafor [c], Akanksha Patel [b], Jiansong Qin [a], Jin Xu [d], Carl Lawton [a], Hsi-Wu Wong [a], Margaret J Sobkowicz [b], Dongming Xie [a*]

[a] Department of Chemical Engineering, University of Massachusetts Lowell, Lowell, MA 01854, USA

[b] Department of Plastics Engineering, University of Massachusetts Lowell, Lowell, MA 01854, USA

[c] Energy Engineering Program, University of Massachusetts Lowell, Lowell, MA 01851, USA

[d] Department of Chemistry, University of Massachusetts Lowell, Lowell, MA 01854, USA

* Corresponding author:

Dr. Dongming Xie, Department of Chemical Engineering, University of Massachusetts Lowell. Phone: +1-978-934-3159; Email: Dongming_Xie@uml.edu.

# Abstract

Poly(ethylene terephthalate) (PET) is one of the world's most widely used polyester plastics. Due to its chemical stability, PET is extremely difficult to hydrolyze in a natural environment. Recent discoveries in new polyester hydrolases and breakthroughs in enzyme engineering strategies have inspired enormous research on biorecycling of PET. This study summarizes our research efforts toward large-scale, efficient, and economical biodegradation of post-consumer waste PET, including PET hydrolase selection and optimization, high-yield enzyme production, and high-capacity enzymatic degradation of post-consumer waste PET. First, genes encoding PETase and MHETase from *Ideonella sakaiensis* and the ICCG variant of leaf-branch compost cutinase ($LCC^{ICCG}$) were codon-optimized and expressed in *Escherichia coli* BL21(DE3) for high-yield production. To further lower the enzyme production cost, a *pelB* leader sequence was fused to $LCC^{ICCG}$ so that the enzyme can be secreted into the medium to facilitate recovery. To help bind the enzyme on the hydrophobic surface of PET, a substrate-binding module in a polyhydroxyalkanoate depolymerase from *Alcaligenes faecalis* (PBM) was fused to the C-terminus of $LCC^{ICCG}$. The resulting four different $LCC^{ICCG}$ variants (LCC, PelB-LCC, LCC-PBM, and PelB-LCC-PBM), together with PETase and MHETase, were compared for PET degradation efficiency. A fed-batch fermentation process was developed to produce the target enzymes up to 1.2 g/L. Finally, the best enzyme, PelB-LCC, was selected and used for the efficient degradation of 200 g/L recycled PET in a well-controlled, stirred-tank reactor. The results will help develop an economical and scalable biorecycling process toward a circular PET economy.



**Keywords:** Poly(ethylene terephthalate), Terephthalic Acid, Biodegradation, Leaf-Branch Compost Cutinase, PETase,

# Graphical Abstract

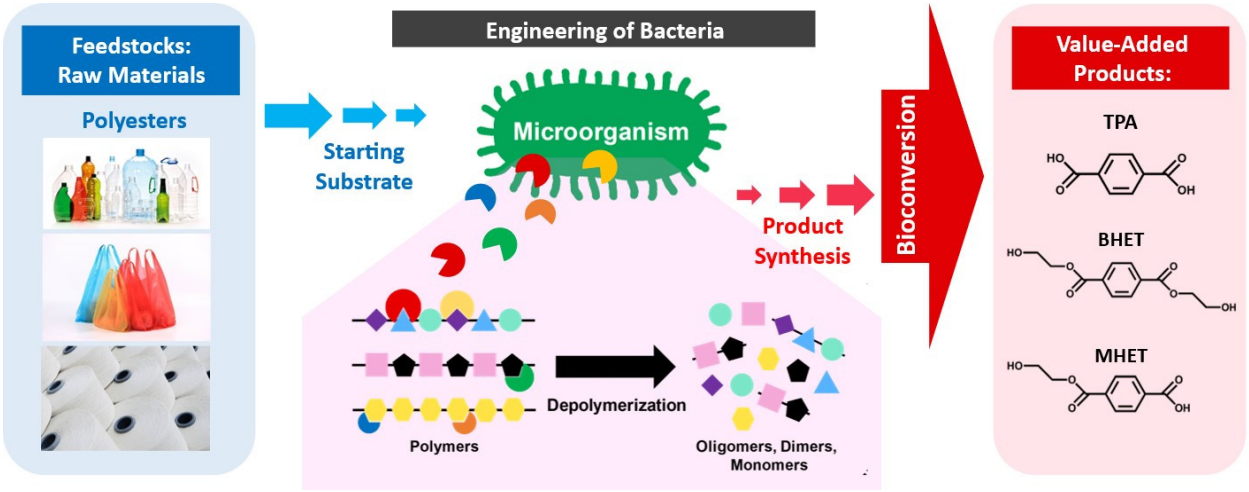

## Introduction

Poly(ethylene terephthalate) (PET) is one of the world's most widely used polyester plastics. PET is durable, transparent, lightweight, non-reactive, thermally stable, cost-effective, exhibiting high-pressure resistance, mechanical strength, and barrier properties (i.e., impermeable to carbon dioxide). While the remarkable material properties make PET a desirable material for applications in food and beverage packaging and the textile industry, they also make PET very challenging to decompose. The demand for PET bottles is continually rising as more bottled beverages are consumed. In 2016, 480 billion plastic bottles were sold in the global market, while 300 billion were sold in 2004 [1]. In addition, 56 million tons of PET were manufactured but only 2.2 million tons were recycled in 2013 [2]. The vast amount of post-consumer PET waste released into the environment harms marine life by entering the food chain [3, 4]. Growing concerns surrounding the environmental impact of post-consumer plastic waste have inspired the search for new technologies and solutions, where microbial biodepolymerization is presently evaluated as a more environmentally friendly strategy for dealing with plastic pollution [5-7].

A variety of bacterial and fungal PET hydrolases have been characterized by actinobacteria and fungi, such as *Thermobifida fusca* [8], *Ideonella sakaiensis* [9, 10], *Fusarium solani* [11-13], and *Humicola insolens* [14]. Advances in metagenomic analysis have created the possibility of obtaining complete or nearly complete genome sequences from uncultured microorganisms, broadening the extent to which genetic information can be explored [15, 16]. A novel gene, encoding a cutinase homolog, with PET degradation activity, leaf-branch compost cutinase (LCC), was cloned from a fosmid library of a leaf-branch compost metagenome by functional screening using tributyrin agar plates [17].

Recently, a gram-negative bacterium, *I. sakaiensis* 201-F6, that can use PET polymer as an energy and carbon source was discovered and isolated [10]. Two important hydrolases to degrade PET were identified, namely the PETase (PET hydrolase) and MHETase (mono(2-hydroxyethyl) terephthalate hydrolase) [18, 19]. The PETase from *I. sakaiensis* and its engineered variants catalyze the degradation of PET polymer into terephthalic acid (TPA), mono(2-hydroxyethyl) terephthalate (MHET), bis(2-hydroxyethyl) terephthalate (BHET), and ethylene glycol (EG) [20]. A mutated *Ideonella* PETase (IsPETase) has been reported to manifest superior thermal stability and higher PET depolymerizability as compared to its wild type counterpart [21]. MHETase further catalyzes the deconstruction of BHET or MHET into TPA and EG. The catalytic activities

of five different cutinases from bacteria *T. fusca* (BTA1 and BTA2), *I. sakaiensis* (PETase), filamentous fungus *F. solani pisi* (FsC), and metagenome-derived LCC have been recently studied on crystalline bottle-grade PET [22] where wild the type LCC outperformed all other evaluated PET hydrolases. Various computational and experimental studies have been performed to study the optimal depolymerization conditions for the development of redesigned PETase variants with improved melting temperatures and enhanced degradation performances at elevated temperatures [20, 23, 24]. In general, the PET degradation rate of wild type LCC (93.2 mg TPA/h/mg enzyme), in the aforementioned study, has outperformed most other enzymes [22]. Owing to the high potential of LCC in degrading persistent semi-aromatic polyesters such as PET, more efforts are being made to seek strategies to make LCC work more efficiently. Detailed structural and functional analysis of LCC has facilitated an understanding of the mechanism by which LCC hydrolyzes PET and thus led to the development of a more efficient enzyme. Several research studies have been accomplished for the improvement of enzymatic PET degradation efficiency and performance by fusing different binding domains to the C-terminus of previously reported variants of LCC [25, 26]. These binding domains, fused to selective PET hydrolases, are able to improve the enzyme sorption at solid-water interface. Therefore, they are considered to be highly effective affinity tags for immobilizing the target enzyme on the surface of the solid substrates, resulting in improved hydrolysis of polymer substrates [27]. The enzyme's activity can be further improved by increasing its thermostability. Tournier et al. generated all possible 209 LCC variants through site-specific saturation mutagenesis [22]. Of those LCC mutant candidates, two variants, namely ICCG (F243I/D238C/S283C/Y127G) and WCCG (F243W/D238C/S283C/Y127G), demonstrated increased deactivation temperatures (thermal tolerance) and significantly increased PET depolymerization [22].

In this study, major PET hydrolases including PETase, MHETase, and $LCC^{ICCG}$ were investigated for the degradation of various PET materials, including extruded post-consumer waste PET flakes, PET powder, and amorphous PET films having different physical properties. The *E. coli* BL21(DE3) strain was employed for the overexpression of desired enzymes, and a fed-batch fermentation process was developed and optimized to achieve high-yield enzyme productions (> 1 g/L). To further improve $LCC^{ICCG}$'s efficiency, new variants of $LCC^{ICCG}$ were generated to improve the secretion of the produced enzyme in fermentation and to enhance the binding efficiency of $LCC^{ICCG}$ on PET surfaces. Finally, the top two $LCC^{ICCG}$ variants (LCC and PelB-

LCC) were used to degrade recycled PET in a scaled-up reactor with a high working capacity (200 g PET/L).

# Materials and Methods

## Strains, Growth, and Culture Conditions

*Escherichia coli* NEB5α was used as the host strain for plasmid construction and propagation. *E. coli* BL21(DE3) was used as the host for protein expression under a T7 promoter. The plasmids used in this study are listed in **Table 1**. All recombinant plasmids were originally derived from low copy number pET-based expression vectors including pET21b(+), pET26b(+), and pET28a(+). The genes of interests inserted into plasmids were under the control of the T7 RNA polymerase promoter.

**TABLE 1. Plasmids used in this study.**

| PLASMID | DESCRIPTION | REFERENCE |
|---|---|---|
| **pLCC** | *Kan*$^R$, pET26b(+) derivative that contained a codon-optimized leaf branch compost cutinase (LCC$^{ICCG}$) variant (F243I/D238C/S283C/Y127G, ICCG) under the control of T7 promoter. | [22] |
| **pPelB-LCC** | *Kan*$^R$, pET26b(+) derivative that a codon-optimized PelB-LCC fused gene which was constructed by fusion of a signal peptide (PelB) of Pectate lyase B (Met1-Ala22) from *Pectobacterium carotovorum* to a LCC$^{ICCG}$ under the control of T7 promoter. | This work |
| **pLCC-PBM** | *Kan*$^R$, pET26b(+) derivative that contained a codon-optimized LCC-PBM fused gene which was constructed by fusion of a linker region from Pro263-Pro287 of 1,4-beta-cellobiohydrolase I from *Trichoderma reesei* and a polyhydroxyalkanoate binding module (Ala428-Pro488) (PBM) of the polyhydroxybutyrate depolymerase from *Alcaligenes faecalis* (GenBank AAA21974.1) to an LCC$^{ICCG}$ under the control of T7 promoter. | This work |
| **pPelB-LCC-PBM** | *Kan*$^R$, pET26b(+) derivative that contained a codon-optimized PelB-LCC-PBM fused gene which was constructed by fusion of a PelB to an LCC-PBM under the control of T7 promoter. | This work |
| **pPETase** | Amp$^R$, pET21b(+) derivative that contained a codon-optimized IsPETase (W159H/S238F) from *Ideonella sakaiensis* 201-F6 under the control of T7 promoter. | [28] |
| **pMHETase** | *Kan*$^R$, pET28a(+) derivative that contained a codon-optimized MHETase gene from *Ideonella sakaiensis* 201-F6 under the control of the T7 promoter. | This work |

**All plasmids were constructed with the addition of a short tract of the poly-histidine tag to the N-terminus or C-terminus to facilitate the enzyme purification*

The plasmid constructs were transformed into *E. coli* strains NEB5α and BL21(DE3) competent cells (New England Biolabs, Ipswich, MA) by the heat shock method. Media and growth conditions for *E. coli* have been previously described by Sambrook and Russell [29]. *E. coli* strains were grown at 30 °C, pH 7.0 with constant agitation speed for shaking at 250 rpm in Luria–Bertani Broth supplemented with 100 µg/mL ampicillin or 50 µg/mL kanamycin. The LB medium contained 10 g/L NaCl (BP 358-212, Fisher Bioreagents), 10 g/L Bacto™ Tryptone (211705), and 5 g/L ultra-pure yeast extract (J850-500G, VWR chemicals).

## Plasmid Construction

**General molecular biology methods**. Restriction enzymes and DNA polymerases were procured from New England Biolabs. Polymerase chain reaction (PCR) amplifications were conducted with Q5 High-Fidelity DNA Polymerase or Taq DNA polymerase at recommended conditions. PCR products and DNA fragments were purified using Monarch® PCR & DNA Cleanup Kit (New England Biolabs). Electrophoresis analysis of the resultant PCR amplicons was carried out in a 1–2% agarose gel. Gel extraction was performed using the QIAquick Gel Extraction kit (Qiagen). Plasmids containing the desired genes were constructed using NEBuilder HiFi DNA assembly cloning kit (New England Biolabs).

## Shake-flask Cultivations of *E. coli* Strains

$LCC^{ICCG}$ [16], PelB-LCC (fused signal peptide of Pectate lyase B (Met1-Ala22) (PelB) to $LCC^{ICCG}$), LCC-PBM (fused polyhydroxyalkanoate binding module (Ala428-Pro488) (PBM) to $LCC^{ICCG}$), PelB-LCC-PBM (fused PelB to an LCC-PBM), PETase (*Is*PETase W159H/S238F), and MHETase were expressed in *E. coli* BL21(DE3) with the corresponding plasmids shown in Figure S4 and Table 1. The *E. coli* cells were grown in ZYM-5052 auto-induction medium, which contained 1% tryptone (gibco Bacto™ Tryptone, Cat. No. 211705), 0.5% yeast extract, 25 mM $Na_2HPO_4$, 25 mM $KH_2PO_4$, 50 mM $NH_4Cl$, 5 mM $Na_2SO_4$, 2 mM $MgSO_4$, 0.2X trace elements, 0.5% glycerol, 0.05% glucose, and 0.2% α-lactose. The final pH of the medium was adjusted to 7.0 using 1M NaOH. A single transformed colony was selected from an LB plate with an appropriate antibiotic for selection and used to inoculate a starter culture in an LB medium. The

starter culture was grown overnight at 30 °C with agitation speed of 250 rpm and was freshly used at a dilution of 1:50 to inoculate expression cultures in the ZYM-5052 auto-induction medium. The expression cultures were grown at 25 °C, 250 rpm for 24 h to achieve maximum enzyme production. Samples were taken sterilely after 0, 3, 6, 12, and 24 h and analyzed for $OD_{600}$. From $OD_{600}$ dry cell weight (DCW, g/L) was calculated by an established correlation (DCW = 0.47 × $OD_{600}$). All flask culture experiments were performed in duplicate.

## 1-L Fed-batch Fermentation of *E. coli* Strains

For seed preparation, *E. coli* strains were cultivated on LB agar plates with antibiotics at 30 °C overnight and one single colony was inoculated to 30 mL LB medium in a 250-mL shake flask to start the first-stage seed culture. When the $OD_{600}$ reached 3-4, 1 mL of the first-stage seed culture was transferred to a 250-mL flask containing 35 mL fresh seed culture medium to grow for another 6 hours until an $OD_{600}$ of 1.5-2.5 was reached. All shake flask cultures were carried out at 30 °C, 250 rpm in a New Brunswick G25 Shaker Incubator. The second-stage seed culture was used to inoculate the 1-liter fed-batch fermentor (Biostat B-DCU, Sartorius, Germany) at 5% (v/v). The exponentially growing cells from the second-stage flask seed culture were transferred into the bioreactor to initiate the fermentation (t = 0 h). The initial fermentation medium (0.7 liters) contained 20 g/L yeast extract, 1.7 g/L citric acid, 14 g/L $KH_2PO_4$, 4 g/L $(NH_4)_2HPO_4$, 0.6 g/L $MgSO_4$, 0.5 g/L NaCl, 11 mg/L $CaCl_2$, 15 g/L glucose, 1X trace metals I, 1mL/L kanamycin, and 1 mL/L antifoam 204 (Sigma, United States of America). The trace metals I (100X) stock solution contained 840 mg/L EDTA, 220 mg/L $CuSO_4 \cdot 5H_2O$, 1500 mg/L $MnCl_2 \cdot 4H_2O$, 250 mg/L $CoCl_2 \cdot 6H_2O$, 300 mg/L $H_3BO_3$, 4 g/L $C_6H_8FeNO_7$, 250 mg/L $Na_2MoO_4 \cdot H_2O$, and 1,300 mg/L $Zn(CH_3COO)_2$. The dissolved oxygen level of the fermentation experiments was set at > 5% of air saturation by cascade controls of agitation speed between 600 and 1200 rpm, gas flow rate between 0.3 - 0.6 vvm, and pure oxygen enrichment (0-50 %). A two-stage temperature control profile was implemented (30 °C for the growth phase during 0-12 h and 25 °C for enzyme production in the remainder of the run) and the pH value was maintained at 7.0 throughout the run by feeding 5M ammonium hydroxide solution. Glucose feeding started as initial glucose was depleted (t = 10-11 h). The glucose feed solution contained 600 g/L glucose, 1M $MgSO_4$, and 1X trace metals II. The trace metals II (100X) stock solution contained 1,300 mg/L EDTA, 370 mg/L $CuSO_4 \cdot 5H2O$, 2,350 mg/L $MnCl_2 \cdot 4H_2O$, 400 mg/L $CoCl_2 \cdot 6H_2O$, 500 mg/L $H_3BO_3$, 4 g/L $C_6H_8FeNO_7$, 400 mg/L

$Na_2MoO_4 \cdot H_2O$, and 1,600 mg/L $Zn(CH_3COO)_2$. Residual glucose concentrations were maintained at limited levels (< 0.1 g/L) during the fed-batch fermentation by using the pre-set feeding profile. Enzyme expression was induced by adding three shots of Isopropyl β-D-1-thiogalactopyranoside (IPTG), *i.e.*, 3 mL, 2.5 mL, and 2.5 mL of IPTG (0.1 M in stock solution) at 11 h, 14 h, and 17 h, respectively, to achieve a total IPTG concentration of 1 mM in the culture medium. For DCW analysis, 5 mL of cultivation broth was washed and centrifuged (4,500 g for 10 min at 4 °C), and then filled into a pre-dried and pre-weighed aluminum weighing dish before drying at 60 °C for 72 h. The *E. coli* fermentation broth was collected and centrifuged (4,500 g for 30 min at 4 °C). Both pellets and supernatants were frozen separately at -20 °C for subsequent product extraction and quantification. For crude enzyme preparation, the *E. coli* cells were disrupted by several freeze/thaw cycles at -80 °C and the cultivation broth was centrifuged (4,500 × g for 30 min at 4 °C). The supernatant containing crude enzymes was harvested.

## Enzyme Extraction and Quantification

Polyhistidine-tagged expressed proteins were collected and purified using the MagneHis™ protein purification system (Promega). The size and molecular weight (kDa) of enzymes were estimated via protein migration in SDS-polyacrylamide gel using XCell SureLock™ electrophoresis tank and the enzyme concentrations were quantified using the Pierce™ Gold BCA protein assay kit to determine the mass concentration (g/L) of enzyme/protein produced.

## Poly(ethylene terephthalate) (PET) Substrates

Post-consumer recycled waste PET flakes (RPET), PET powder (PPET, Goodfellow), and amorphous PET film (AmPET, Goodfellow) were used as substrates for the enzymatic degradation of PET in this study. The Extruded RPET (ExPET) was obtained by extrusion of RPET using twin screw extrusion at 200 rpm with a throughput of 9 g/min (15 mm diameter screws 60:1 L:D, Technovel Japan) [30]. The types of poly(ethylene terephthalate) (PET) materials used in this study and their properties are listed in **Table 2**. Glass transition temperature ($T_g$), melting temperature ($T_m$), and crystallinity (%) values were acquired using Differential Scanning Calorimetry (DSC) analysis. Number average and weight average molecular weight (i.e., Mn and Mw, respectively) for PET substrates was determined using Gel Permeation Chromatography (GPC). Detailed protocols for DSC and GPC analysis are provided in the Supplementary

Information. However, intrinsic viscosity (IV) measurements were carried out using Ubbelohde Viscometer by adding o-chlorophenol as a solvent. Billmeyer's relationship, as described in Supplementary Information, was used to determine IV values for PET substrates.

**TABLE 2. Types of poly(ethylene terephthalate) (PET) used in this study.**

| Abbreviation | Description | Manufacturer | $T_g$ (°C) | $T_m$ (°C) | Crystallinity | IV | $M_n$ (kDa) | $M_W$ (kDa) | PDI |
|---|---|---|---|---|---|---|---|---|---|
| **RPET** | Recycled PET bottle flakes acquired after washing/shredding | Post-consumer from UltrePET | 81.8 | 244.5 | 30.5% | 0.75 | 35.9 | 68.7 | 1.91 |
| **PPET** | PET powder, copolymer with 1ppm Acetaldehyde, 300 µm | Goodfellow | 74.2 | 244.1 | > 40% | 0.8 | 27.3 | 52.0 | 1.91 |
| **ExPET** | Extruded RPET | Post-consumer from UltrePET | 67.9 | 251.9 | 7% | 0.38 | 17.6 | 44.3 | 2.51 |
| **AmPET** | Amorphous PET film, 0.25 mm | Goodfellow | 69.7 | 250.2 | 2-5% | 0.75 | – | – | 1.58 |

The RPET flake used in this study was obtained from UltrePET, LLC. (Albany, New York), which has a number average molecular weight ($M_n$) of 24,5 00 g/mol, a melting point ($T_m$) of 244.5 °C, a glass transition temperature ($T_g$) of 81.8 °C, and a 30.5% crystallinity. An ultra-high twin screw extruder (Technovel Corporation Osaka, Japan) was used for the reactive processing of RPET flakes. A mechanical grinder (Wiley Mill grinder) was used to mill the extruded samples into small particles, which were then sieved using a Rotap sieve shaker for further analysis and degradation studies. The PET materials were ground into particles with Mesh-40 and -60 sizes, which correspond to maximum particle sizes of 0.4 mm and 0.25 mm, respectively. The intrinsic viscosity (IV) and $M_n$ of the extruded samples were calculated using o-Chlorophenol (Sigma-Aldrich). The experimental protocols for reactive extrusion setup and RPET particle preparation are included in the supplementary information.

## PET Depolymerization in 15-mL tube reaction

**Using PPET or RPET as Substrate**: The enzymatic reactions were carried out in 15 mL glass tubes, with each containing 5 mg PPET or RPET (40 mesh or 60 mesh size) and 1 mL of

protein-specific buffer, i.e., 100 mM potassium phosphate buffer (pH 8.0) for $LCC^{ICCG}$ variants and 50 mM glycine-sodium hydroxide (pH 9.0) for *Is*PETase (W159H/S238F) and MHETase. The depolymerization was initiated by adding the purified enzyme ($LCC^{ICCG}$ variant, *Is*PETase, or *Is*PETase + *Is*MHETase) to a final concentration of 0.1 μM. The tube reactions were conducted without pH control at 40 °C for PETase and PETase + MHETase and 65 °C for LCC with an agitation of 250 rpm in a water-bath shaker for 48 h. Samples were harvested at multiple time points and analyzed by thin-layer chromatography (TLC) or high-performance liquid chromatography (HPLC) to determine PET depolymerization kinetics. Samples taken for HPLC and TLC analysis were quickly quenched using equal volume of methanol for immediate termination of the depolymerization reaction. PET degradation was observed at 40X magnification under a light microscope. Assays were performed in duplicates and evaluated accordingly.

**Using AmPET or ExPET as Substrate:** The enzymatic reactions were carried out in 15 mL glass tubes, with each containing either 10 mg AmPET + 2 mL potassium phosphate buffer (100 mM, pH 8.0) or 2.5 mg ExPET + 1 mL potassium phosphate buffer (100 mM, pH 8.0). The depolymerization was initiated by adding the purified $LCC^{ICCG}$ variant to a final concentration of 0.1 μM. The tube reactions were conducted without pH control at 65 °C with an agitation of 250 rpm in a water-bath shaker for 10 days. Samples were harvested at multiple time points and quenched using an equal volume of methanol to immediately terminate the reaction. Harvested and quenched samples were then analyzed by HPLC to determine PET depolymerization kinetics. PET degradation was observed at 40X magnification under a light microscope. Assays were performed in duplicates and evaluated accordingly.

**PET Depolymerization in 1-L reactor**

The enzymatic degradation of PET was scaled-up in a 1-L bioreactor (BIOSTAT® B-DCU, Sartorius, Germany). Prior to the 1-L reactor experiments, the recycled PET (RPET) rods with a crystallinity within 10-12% and diameters of 1-2 mm were ground into pellets with particle sizes ≤ 2 mm. The reaction medium (0.5 L) contained 200 g/L RPET pellets in the 100 mM potassium phosphate buffer (pH 8.0). The pH meter was calibrated using standard pH 4.0 and pH 7.0 buffers. The reaction was initiated by adding the purified $LCC^{ICCG}$ or PelB-LCC enzyme to the reaction medium to a final concentration of 2 μM which corresponds to ratios of 0.29 mg LCC/g PET or 0.31 mg PelB-LCC/g PET, respectively. The reactor's temperature was controlled at 65 °C and the pH value was maintained at 8.0 by cascade control with the addition of KOH (10 M). The

agitation speed was maintained at 200 rpm throughout the experiment using a single six-blade, Rushton-type impeller to provide efficient mixing in the reactor.

Samples of 5 mL were collected every 2-12 h from the reaction at different time points using the sterile syringe for further HPLC analysis. An equal volume (5 mL) of tetrahydrofuran (THF) was immediately added to each sample right after collection, to quickly quench the reaction. These samples were then diluted using 100 mM potassium phosphate buffer (pH 8.0) to determine the amount of TPA and BHET produced from the degradation of PET pellets using HPLC.

## Analytical Methods for TPA, MHET, BHET Detection and Quantification

**Thin-Layer Chromatography (TLC)**: TLC, as a qualitative technique, was used to separate TPA from untreated and degraded PET samples and performed directly on the spots of TLC aluminum sheets (silica gel 60 $F_{254}$) (Millipore-Sigma). The same samples analyzed by TLC were also analyzed by HPLC. The solvent for TPA detection and separation on the TLC plate was prepared by mixing methanol: deionized water: 7.6% hydrochloric acid (by dissolving 37% HCl in methanol) in the ratio of 18: 2: 0.15 (v/v/v), respectively. After developing the TLC plate, the TPA spots were detected using a 254 nm UV lamp.

**High-Performance Liquid Chromatography (HPLC)**: The concentrations of TPA, MHET, and BHET in samples were quantified by HPLC to determine the extent of PET depolymerization. When required, samples were diluted in 100 mM potassium phosphate buffer at a pH of 8.0. Then, 500 µL of methanol was added to 500 µL of sample dilution. After homogenization and filtering through a 0.25 µm syringe filter, samples were injected into Agilent 1100 Series HPLC system (Agilent Technologies, Palo Alto, CA) equipped with a pump module, an autosampler, a column oven, and a UV absorbance detector.

The separation of the sample mixtures was achieved using a Luna® C18(2) LC column (150 × 4.6 mm, 5 µm) (Phenomenex, Torrance, CA). The mobile phase consisted of deionized water with 20 mM $H_2SO_4$ (A), and methanol (B), which were eluded using the following gradient: 80% A and 20% B to 35% A and 65% B in 15 min, back to 80% A and 20% B in 5 min, and held at the composition for another 5 min. The flow rate was adjusted to 0.6 mL/min. The temperature was held constant at 40 °C. The injection volume was 1.5 µL. The chromatograms were acquired at 240 nm. The TPA, MHET, and BHET peak areas were calibrated using solutions prepared by commercial TPA (Acros Organics, Geel, Belgium) and BHET (TCI, Tokyo, Japan) and MHET

synthesized in-house. Typical HPLC chromatograms and the retention times for standard TPA, MHET, BHET and real reaction samples are shown in **Figure S1** in Supplementary Information. Sample quantification assays were performed in triplicates and evaluated accordingly.

These HPLC results were then utilized to determine the percentage degradation efficiency of PET into TPA, MHET, and BHET by using the **Equation (1)**, which considers the depolymerization of PET into its all three possible monomer products (TPA, BHET, or MHET). Since the repeating unit of PET has a molecular weight of 192 g/mol and the molecular weights of the monomers TPA, MHET, BHET are 166 g/mol, 209 g/mol, and 254 g/mol, respectively, the overall PET degradation efficiency can be calculated as:

$$Degradation\ Efficiency\ (\%) = \frac{TPA\ (g)\frac{192}{166} + MHET\ (g)\frac{192}{209} + BHET\ (g)\frac{192}{254}}{Total\ PET\ loaded\ (g)} \times 100\% \quad (1)$$

# Results

## Expression of PETase, MHETase, and LCC$^{ICCG}$ variants in *E. coli* BL21(DE3)

The *E. coli* BL21(DE3) with a T7 RNA polymerase-based expression system was used to overexpress the re-engineered PETase (*Is*PETase W159H/S238F) and MHETase with enhanced efficiency [28]. After that, the expression system was further used to express the LCC$^{ICCG}$ [22] and its variants to degrade PET more efficiently than PETase and MHETase. To promote the production of LCC in the culture medium, the secretion of recombinant proteins in the periplasmic space or extracellular environment offers a potential advantage [31]. Thus, an N-terminal PelB signal peptide, leader sequence of pectate lyase B (Met1-Ala22) from *Pectobacterium carotovorum*, was attached to the LCC to direct the protein to the outer membrane through the Sec-dependent pathway. Recombinant proteins were produced as LCC without the signal peptide or with the N-terminal PelB (PelB-LCC). Since binding the enzyme to the surface of PET may help initiate the degradation process, the substrate-binding modules (polymer-binding domain, PBM) of a polyhydroxyalkanoate depolymerase from *Alcaligenes faecalis*, together with the linker (2.3 kDa) from a cellobiohydrolase from *Trichoderma reesei*, [32, 33] was fused to the C-terminus of LCC to improve enzyme adsorption to the PET substrate. Therefore, four LCC$^{ICCG}$ constructions (namely LCC, PelB-LCC, LCC-PBM, and PelB-LCC-PBM) were generated and compared for PET degradation. Plasmids containing the genes encoding PETase, MHETase, LCC, PelB-LCC,

LCC-PBM, and PelB-LCC-PBM were constructed separately with the addition of a short tract of the poly-histidine tag to the N-terminus or C-terminus to facilitate the enzyme purification. The *E. coli* BL21(DE3) cells harboring corresponding plasmids were grown in shake flasks for producing the target enzymes, which were purified through an immobilized metal affinity chromatography (IMAC) and verified by SDS-PAGE.

As shown in the non-reducing SDS-PAGE gel pictures in **Figures 1(e)**, **2**, and **S2**, the *E. coli* cells successfully produced all the target enzymes (LCC: 29 kDa; PelB-LCC: 31 kDa; LCC-PBM: 37 kDa; PelB-LCC-PBM: 40 kDa; PETase: 36 kDa; MHETase: 52 kDa) in the shake flask cultures. In addition, it appeared that some of the produced PETase and MHETase were leaked into the culture medium after the IPTG induction for 20 h, suggesting that some cell lysis might have taken place due to the possible toxicity of PETase or MHETase to the *E. coli* cells.

## High-Yield Production of PETase and LCC$^{ICCG}$ Variants in Fed-Batch Bioreactor

Based on the recent techno-economic analysis by the National Renewable Energy Laboratory (NREL) [34], a significant portion of the cost of the recycled TPA from the enzymatic PET hydrolysis process is due to the enzyme cost. The results suggested that increasing the enzyme loading from 1 to 10 mg/g PET may lead to an 11% higher total cost [34]. Therefore, reducing the enzyme production cost is important to a commercially viable PET enzymatic hydrolysis process. In addition to the earlier effort of using PelB signal peptide to help secrete the produced target protein, we further optimized the fed-batch fermentation conditions, including the temperature profile, glucose feeding strategy, and IPTG induction for protein expression, to achieve the highest production of PETase, MHETase, and four LCC$^{ICCG}$ variants (LCC, PelB-LCC, LCC-PBM, and PelB-LCC-PBM) with the *E. coli* BL21(DE3) expression systems, as described in the fed-batch fermentation protocols. All enzyme expressions were induced by adding three shots of IPTG during 11~17 h for a total of 0.1 M in the fermentation medium.

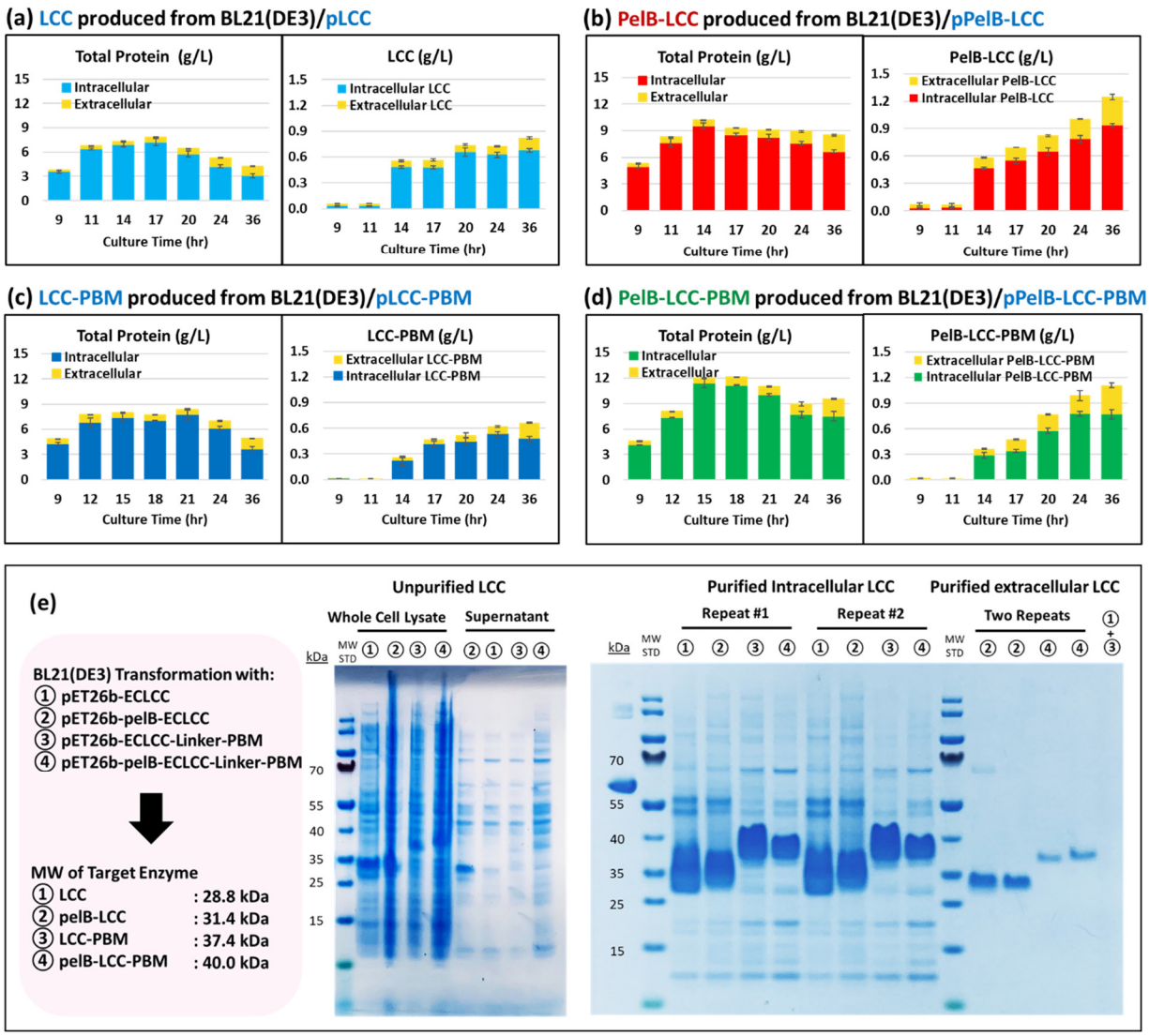


**FIGURE 1.** Production of LCC$^{ICCG}$ enzymes (LCC, PelB-LCC, LCC-PBM, PelB-LCC-PBM) from fermentation of *E. coli* BL21(DE3) under 1-L fed-batch bioreactor conditions. **(a) - (d)** Time courses of intracellular and extracellular total protein and purified LCC, PelB-LCC, LCC-PBM, and PelB-LCC-PBM, respectively. **(e)** Non-reducing SDS-Page gel results of the samples of whole cell lysate, supernatant, and purified LCC$^{ICCG}$ enzymes from both cell pellets (intracellular LCC$^{ICCG}$) and supernatant (extracellular LCC$^{ICCG}$). The *E. coli* BL21(DE3) was transformed with the plasmid pLCC, pPelB-LCC, pLCC-PBM, or pPelB-LCC-PBM, respectively, for the production of corresponding LCC$^{ICCG}$ variants. Enzyme expression was induced by adding three shots of IPTG during 11~17 h for a total of 0.1 M in the fermentation medium. Note: The non-reducing SDS-PAGE results of LCC and PelB-LCC may give higher molecular weights than expected because their 3D structures retain disulfide bond.

The produced enzymes PETase (*Is*PETase W159H/S238F), MHETase, and four LCC$^{ICCG}$ variants (LCC, PelB-LCC, LCC-PBM, and PelB-LCC-PBM) were purified. The concentrations of total proteins and purified enzymes were quantified by using Pierce™ Gold BCA protein assay kit, as described in the protocols. These purified enzymes were further tested and compared for their PET depolymerization activities with various PET materials to identify the best enzyme. **Figure 1** shows the production of the total protein and the target enzyme for all four LCC$^{ICCG}$ variants under the optimized fed-batch fermentation conditions. For all four strains, the total protein production reached the peak values (7-12 g/L) at around 18 h, which was about 6 hours after the first IPTG induction. After that, the total protein production started to decline. It appeared that the PelB signal peptide for LCC secretion helped increase total protein production. The strain expressing PelB-LCC-PBM produced the highest total protein (12 g/L), followed by the strain expressing PelB-LCC (9.5 g/L). Among all the total protein produced, about 10-15% was the target LCC enzyme. PelB-LCC was produced at the highest concentration (1.2 g/L or 38 μM), followed by PelB-LCC-PBM (1.1 g/L or 28 μM), LCC (0.8 g/L or 28 μM), and LCC-PBM (0.6 g/L or 16 μM), respectively. Unlike the total protein productions, which had a peak concentration at approximately 18 h, all LCC concentrations continued to increase until the end of the run. The PelB secretion peptide indeed helped the *E. coli* strains secrete more extracellular LCC enzymes, which contributed to about 30% of the total PelB-LCC and PelB-LCC-PBM produced **(Figure 1 b and d)**. However, for LCC and LCC-PBM about 10-15% was also produced extracellularly **(Figure 1 a and c)**. A similar study has been conducted to improve the secretion efficiency of PETase by *E. coli BL21* using PelB signal peptide [31]. However, the secretion efficiency and PET degradation capability reported in that study were not as high as observed by our *E. coli* strains that secreted more extracellular LCC enzyme with a contribution to about 30% of the total targeted LCC enzyme for significantly improved PET degradation capabilities. Probably due to cell lysis, as indicated by the cell density decline in **Figure S3 (a)**, some proteins were released from the cells for strains without expressing the PelB signal peptide. The produced LCC enzymes were confirmed with the non-reducing SDS-PAGE gel analysis (**Figure 1 e**).

The total protein and PETase production for strain *E. coli* BL21(DE3)/pPETase under the 1-L fed-batch fermentation conditions was shown in **Figure 2**. The total protein production reached the maximum value (5 g/L) at 16.5 h, and the PETase concentration continuously increased to 0.4 g/L at around 24 h and remained constant until the end of the run. As indicated by the extracellular

portion in **Figure 2 (a) and (b)**, up to 30% of the total protein or PETase was released into the medium in the late stage of the fermentation due to cell lysis. It seems that PETase is more toxic to the *E. coli* cells as compared to LCC$^{ICCG}$ variants (LCC, PelB-LCC, LCC-PBM, and PelB-LCC-PBM), thus the cell density (**Figure S3 b**), total protein, and target enzyme production were all lower than those achieved in the experiments with the *E. coli* strains expressing LCC enzymes (**Figure 1**). The lower cell density as shown in **Figure S3 (b)** clearly supports the claim of the increased toxicity from PETase. The produced PETase was also confirmed by SDS-PAGE for the samples of whole-cell lysate and purified PETase (**Figure 2 c**).

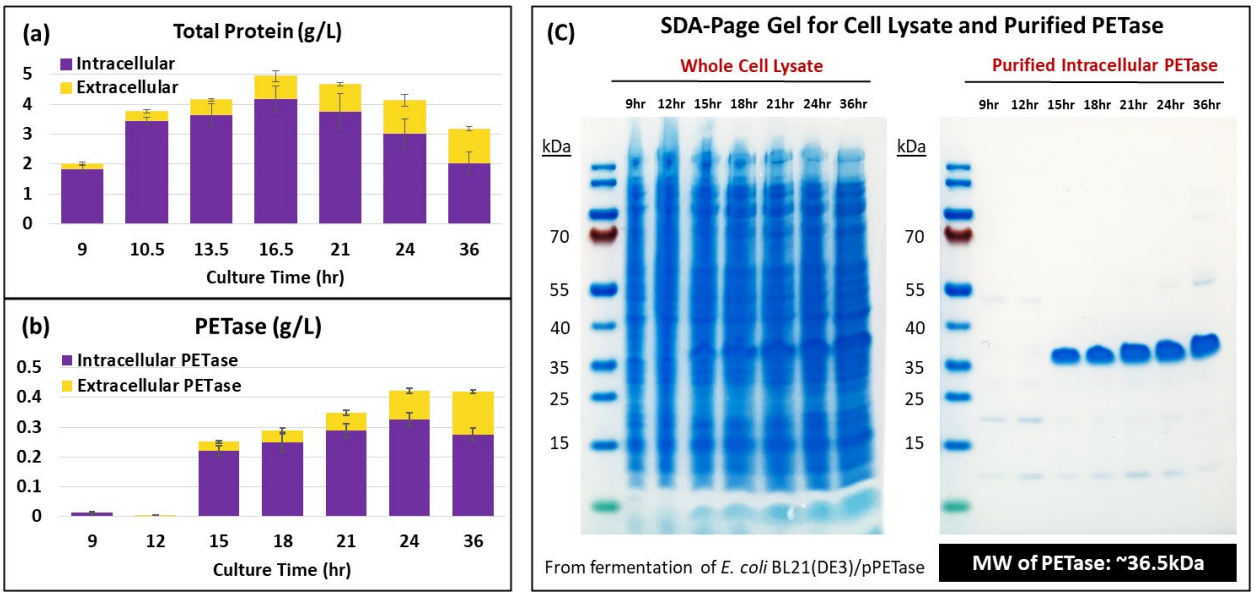


**FIGURE 2.** Production of PETase from the fermentation of *E. coli* BL21(DE3) under 1-L fed-batch bioreactor conditions. **(a)** Total intracellular and extracellular protein produced by *E. coli* BL21(DE3)/pPETase; **(b)** Intracellular and extracellular PETase produced by *E. coli* BL21(DE3)/pPETase; **(c)** The non-reducing SDS-Page gel results of the samples of whole cell lysate and purified intracellular PETase enzymes from both cell pellets (intracellular PETase) and supernatant (extracellular PETase).

## Comparison between LCC, PelB-LCC, LCC-PBM, and PelB-LCC-PBM

To increase the binding efficiency of the PET hydrolase to the PET substrate surface, a PBM (6.3 kDa) was designed to attach to the LCC$^{ICCG}$ by a linker sequence (2.3 kDa). The cutinases fused to the binding module were compared to the original LCC$^{ICCG}$ enzymes in terms of affinity towards the hydrophobic substrates, PET substrate from post-consumer bottle scraps, and commercial PET powders. Binding efficiency of enzyme with PET substrate was estimated in

accordance with the difference between the final and initial concentration of free enzyme in the buffer solution, along with PET substrate, after certain reaction time. In both cases, the adsorption of PBM-containing enzymes, *i.e.*, LCC-PBM and PelB-LCC-PBM, almost doubled the binding efficiency on PET films and PET powders as compared to the cutinases without binding domains (LCC and PelB-LCC) **(Figure 3 a)**.

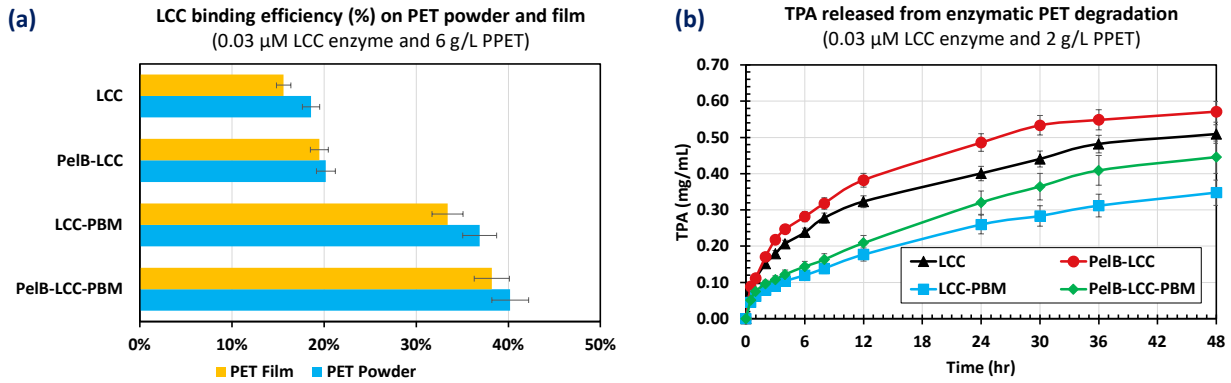


**FIGURE 3.** Comparison between the four LCC$^{ICCG}$ variants (LCC, PelB-LCC, LCC-PBM, and PelB-LCC-PBM) for PET degradation and enzyme binding efficiency (%) on PET. **(a)** Binding/adsorption efficiency (%) of four LCC$^{ICCG}$ variants on PET powder (Goodfellow) and film; enzyme and substrate loading: 0.03 mg enzyme /g **PET**; error bar: triplicate reaction. **(b)** TPA is produced from the degradation of PET powder (Goodfellow) with four different LCC$^{ICCG}$ variants. The experiments used 0.03 µM LCC enzyme and 2 g/L PPET; buffer loading: 100 mM potassium phosphate buffer (pH 8.0); reaction temperature: 65 °C.

The use of PBM links containing the hydrophobic nature contributed to increased binding efficiency on the surface of PET. This relevance of enzyme adsorption for efficient hydrolysis of polymers by fusing PBM with the native enzyme has also been reported in literature [33]. However, The PET degradation efficiencies were PelB-LCC > LCC and PelB-LCC-PBM > LCC-PBM based on the TPA released from the reaction (**Figure 3 b**). It appeared that the improved binding on the PET surface with PBM failed to improve the PET degradation. Interestingly, the PelB signal peptide for protein secretion significantly improved the PET degradation as PelB-LCC > LCC and PelB-LCC-PBM > LCC-PBM, as seen in **Figure 3 (b)**. In addition, the PelB peptide slightly improved the binding efficiency of the enzyme on PET surface (**Figure 3 a**). It is still unclear whether binding the enzyme to the PET surface is critical to the enzymatic degradation process.

## Identify the Best PET Hydrolase for Biodegradation of PET

Various PET materials were further tested to identify the best enzyme from the candidate group of LCC, PelB-LCC, LCC-PBM, PelB-LCC-PBM, PETase, and PETase + MHETase. Commercial PET powders (PPET, Goodfellow) with particle sizes < 0.3mm and crystallinities > 40%, mesh-40 recycled PET (RPET) particles with sizes < 0.4 mm and crystallinities of 28.2%, mesh-60 RPET particles with sizes < 0.25 mm and crystallinities of 30.5% were used as the feedstocks **(Figure 4 a)**. TPA generated from the PET degradation experiments within 48 h was rapidly confirmed by TLC (**Figure 4 b** and **c**). Then the produced TPA using four $LCC^{ICCG}$ variants, PETase, PETase + MHETase was further analyzed by HPLC and the degradation efficiencies are shown in **Figure 4 d** and **e**.

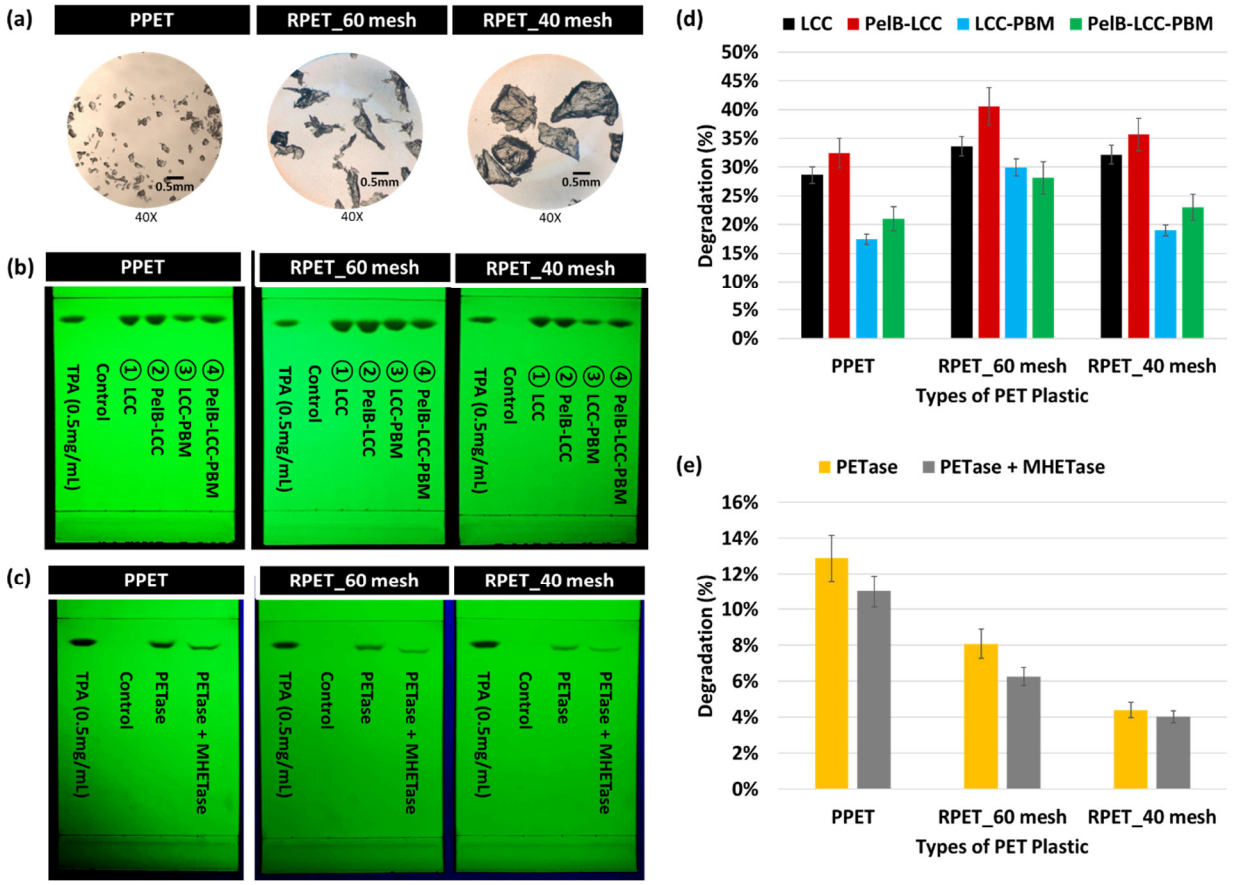


**FIGURE 4.** Catalytic activities of $LCC^{ICCG}$ variants on PET powder (PPET) or recycled PET (RPET) flakes. **(a)** PPET, RPET_60 mesh, and RPET_40 mesh particles observed under a microscope; **(b)** Degradation of PPET, RPET_60 mesh and RPET_40 mesh particles with $LCC^{ICCG}$ variants; **(c)** Degradation of PPET, RPET_60 mesh and RPET_40 mesh particles with PETase and MHETase; **(d)** PET degradation efficiency (%) for $LCC^{ICCG}$ variants based on produced TPA; **(e)** PET degradation efficiency (%) for PETase and

PETase + MHETase based on the produced TPA. The TPA released from PET was analyzed by TLC for (b) and (c) and further quantified with HPLC for (d) and (e). Enzyme loading: 0.1 μM; substrate loading: 5 mg/mL; buffer: 100 mM potassium phosphate buffer (pH 8.0); reaction temperature: 65 °C.

As shown in **Figure 4 b and d**, The RPET samples with 60 mesh sizes (≤ 0.45 mm) had higher degradation rates than the samples with 40 mesh sizes (≤ 0.7 mm) for all the enzymes investigated. Several studies have been reported suggesting the higher initial enzymatic depolymerization rate for substrate with higher surface area and smaller particle size as compared to substrates with lower surface area [35, 36]. It was observed that the smaller particles of PET had higher specific surface area, which was more beneficial for the enzymatic degradation process. TPA production from PPET (≤ 0.30 mm), however, was comparable to that from RPET_40 mesh (≤ 0.45 mm). The higher crystallinity in PPET increased the difficulty in enzymatic degradation, though PPET has the smallest particle size [37]. Among all four $LCC^{ICCG}$ variants/constructions, PelB-LCC led to the highest TPA production, followed by LCC, PelB-LCC-PBM, and LCC-PBM. The results were consistent with our early investigation, as seen in **Figure 3 (b)**, i.e., the PelB peptide improved PET degradation as well as protein secretion. Although the adsorption to PET by the LCC-PBM and PelB-LCC-PBM fusion enzymes was significantly enhanced as compared with LCC and PelB-LCC, their catalytic activities on PET substrates were not as competitive (**Figure 3 b**, **Figure 4 d**).

The PETase and the PETase + MHETase produced from *E. coli* BL21(DE3) were also tested for PET degradation. Overall, the performance of PET hydrolysis using any $LCC^{ICCG}$ variants was much higher than that using PETase and MHETase from *I. sakaiensis* 201-F6 **(Figure 4 d and e)**. About 12% degradation by PETase was obtained from the provided PPET after 48 hours. PETase has an optimal operating temperature of around 40°C, which is relatively low compared to the glass transition temperature ($T_g$) of PET, which is around 70 ºC [38]. However, all $LCC^{ICCG}$ variants showed the highest activities at 65°C, which is close to PET's glass transition temperature $T_g$. It appeared that the lower thermotolerance of PETase and its optimum working temperature (40 ºC) far lower than $T_g$ may have limited the enzyme's degradation activity. Further engineering of PETase for higher thermotolerance (65 ºC or higher) may be helpful to significantly improve its degradation capability at a large scale [23, 39]. In addition, the substrates treated with PETase and MHETase cocktail exhibited lower levels of TPA production than those only treated with

PETase (**Figure 4 e**). These results were different from what was reported earlier [10, 28]. The MHETase produced from the *E. coli* system may need to be further optimized and purified for future studies.

## Degradation of Low-crystallinity PET with PelB-LCC in 15-mL tube reaction

As demonstrated earlier (**Figure 3 b** and **Figure 4 d**), PelB-LCC was the most efficient enzyme for PET degradation among all four investigated $LCC^{ICCG}$ constructs. It was further used to examine its catalytic activities for two lower-crystallinity PET materials: circular amorphous PET films (crystallinity 2-5%, diameter ~12 mm, thickness ~0.5 mm) and extruded amorphous PET strands (crystallinity ~7%, length ~5 mm, diameter ~0.25 mm). The results showed that ExPET strands were completely degraded after being treated with PelB-LCC for 72 hours while the AmPET films were nearly completely degraded **(Figure 5 a and b)**. For the circular AmPET films, the edges remained undegraded after the enzymatic hydrolysis for 120 hours. The edges of the films, created via mechanical forces, looked opaque and may have higher crystallinity, which may have caused the slow degradation (**Figure 5 a**). The ExPET strands, however, had very minimal rough edges, and thus showed almost complete degradation after 72 hours (**Figure 5 b**). The results were further confirmed by direct weight loss measurements (**Figure 5 c**) and the calculated degradation efficiency based on the TPA yields determined by the HPLC (**Figure 5 d**). In addition, the AmPET films treated with purified PelB-LCC showed a slower degradation efficiency in the beginning as compared to the ExPET strands. The primary reason was that the AmPET films have much smaller specific surface areas than the ExPET strands. The degradation rate of the AmPET films eventually caught up after three days, probably because enzymatic degradation in the early stages created more holes and uneven surfaces, which helped open more surfaces available for accelerating the degradation process. This was verified by the observations of the reacting PET samples under the microscope, where prominent pitting was observed on the surfaces of both AmPET films and ExPET strands (**Figure S5**).

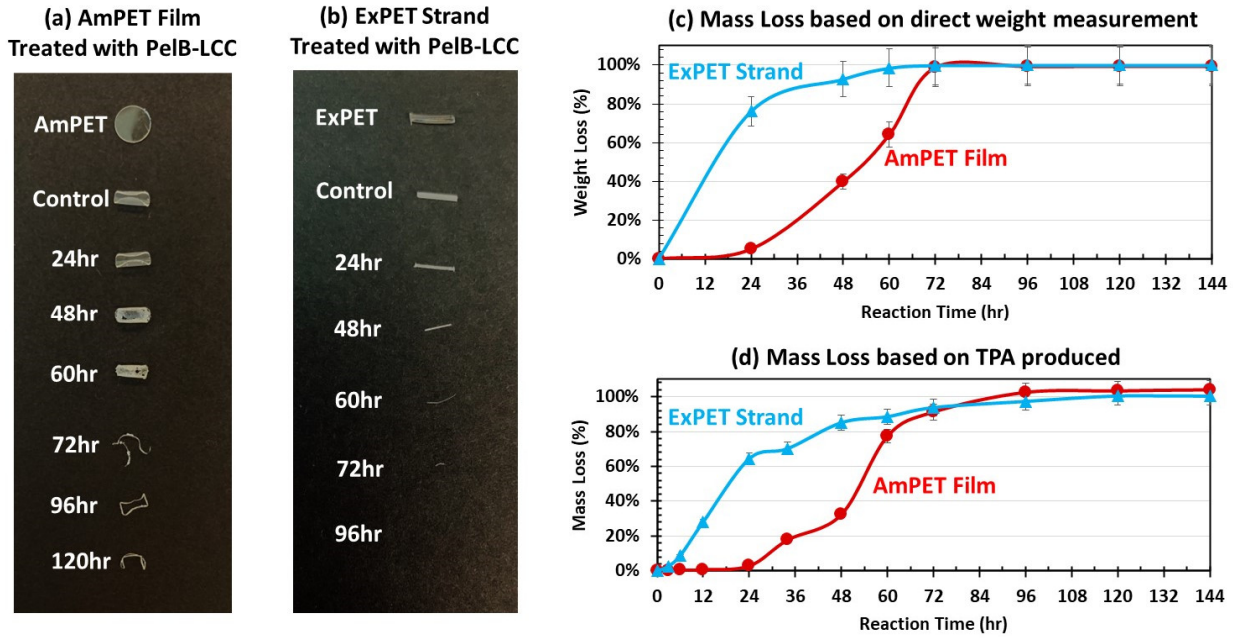


**FIGURE 5.** Biodegradation of AmPET films (crystallinity 2-5%, circular film with a diameter ~12 mm and a thickness ~0.5 mm) and ExPET strands (crystallinity ~7%, short string with a length ~5 mm and a diameter ~0.25 mm) with PelB-LCC. **(a)** Pictures for AmPET film sample during the biodegradation process; **(b)** Pictures for ExPET strand sample during the biodegradation process; **(c)** Weight loss (%) during the biodegradation process; **(d)** Mass loss (%) determined by the produced TPA concentrations (analyzed by HPLC) (i.e., the calculated degradation efficiency % based on the TPA, MHET, and BHET produced). Enzyme loading: 0.1 μM purified PelB-LCC; substrate loading: 5 mg/mL AmPET or 2.5 mg/mL; buffer loading: 100 mM potassium phosphate buffer (pH 8.0); reaction temperature: 65 °C.

## Scale-up of the degradation of recycled PET in 1-L reactor

To scale up the developed enzymatic PET degradation process, the enzymatic reaction was further carried out in a 1-L bioreactor system with temperature, pH value, and agitation speed controlled at 65 ºC, pH 8.0, and 200 rpm, respectively. Recycled PET (RPET) materials in rod (with a crystallinity of ~12%) were extruded into pellets (as described by the protocols provided in Supplementary Information), with most of them having sizes within 1-2 mm (**Figure 6 a**) and loaded to the reaction medium at an initial concentration of 200 g/L. Based on the enzyme activity results from the 15 mL tube scale reactions, the top two $LCC^{ICCG}$ variants, namely LCC and PelB-LCC, were selected as candidates for the scale-up (1-L reactor) experiments. The LCC enzymes

were added into the reactor to a concentration of 2 µM, which corresponded to enzyme/substrate ratios of 0.29 mg LCC/g PET and 0.31 mg PelB-LCC/g PET, respectively.

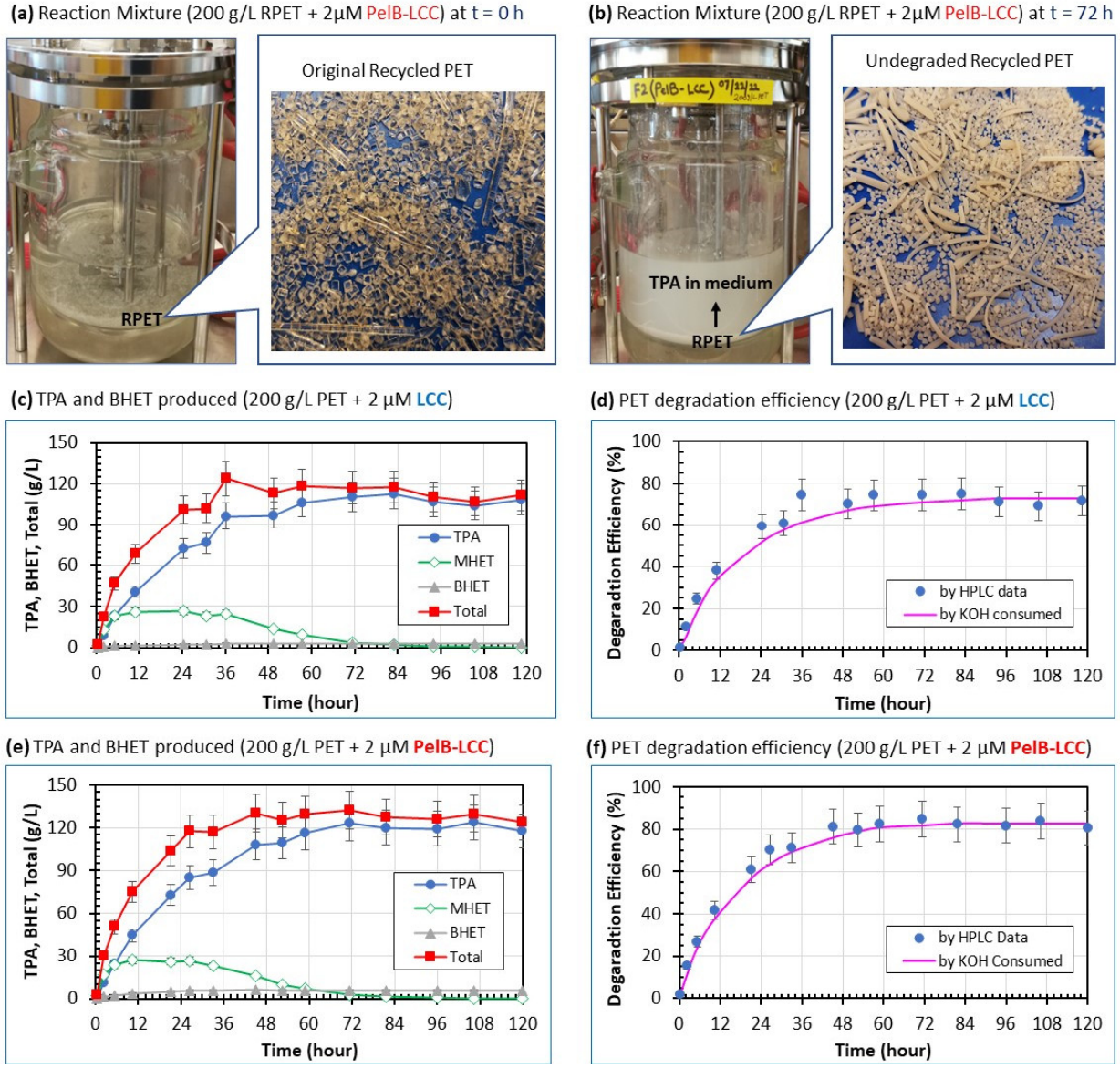


**FIGURE 6.** Scaled-up degradation of recycled PET pellets (with particle sizes of ~2 mm) in a 1-L bioreactor with 200 g/L PET and 2 µM LCC (0.29 mg enzyme/g PET) or PelB-LCC (0.31 mg enzyme/g PET). (a) the reactor and the PET material at t = 0 h, (b) the reactor and the leftover PET material (undegraded) at t = 72 h, (c) TPA, MHET, and BHET produced during the reaction with LCC (determined by HPLC), (d) PET degradation efficiency (%) for the reaction with LCC by estimation with total KOH used to neutralize the produced TPA or by calculation with TPA, MHET, and BHET measured by HPLC, (e) TPA, MHET, and BHET produced during the reaction with PelB-LCC (determined by HPLC), (f) PET

degradation efficiency (%) for the reaction with PelB-LCC by estimation with total KOH used to neutralize the produced TPA or by calculation with TPA, MHET, and BHET determined by HPLC.

Consistent with what was observed earlier in tube reaction experiments (**Figure 3 b**), PelB-LCC demonstrated more efficient degradation of the recycled PET in the 1-L reactor than LCC, within three days which achieved 80% and 70% degradation, respectively (**Figure 6 d** and **f)**. TPA was observed to be the overall major degradation product along with the minimal production of BHET. During the depolymerization process of PET, it was observed that MHET was produced as an intermediate product, and mainly accumulated during the first three days (**Figure 6 c** and **e**). After that, it was further converted into TPA, which is the primary product of our interest. In both scaled-up reaction experiments, the raw PET pellets were depolymerized very quickly at the beginning of the reaction, but the depolymerization rate started to slow down with no significant degradation seen after 72 h. While the original PET pellets looked transparent (**Figure 6 a**), the residual pellets (undegraded PET) after 72 h were typically seen in reduced sizes and looked white and opaque (**Figure 6 b**). Further DSC analysis of the undegraded PET materials showed a significantly increased crystallinity (up to 30%), which may be one of the major reasons that caused the extremely slow degradation after 72 h. In addition, it was observed that the produced TPA had a low solubility in the aqueous reaction medium (< 10 g/L) under pH 8.0 as gradually increased tiny, white suspensions/precipitations were seen in the reactor during the reaction (**Figure 6 b**), which may be caused by accumulation of TPA (> 100 g/L in the late stage).

## Discussion

The cutinase-like enzyme from the leaf-branch compost cutinase, LCC, is a good candidate for biodegradation of post-consumer PET waste. In this study, $LCC^{ICCG}$ [22] demonstrated significantly higher degradation efficiency for several PET materials from different sources than PETase from *I. sakaiensis* [10, 28]. Four variants of $LCC^{ICCG}$, namely LCC, PelB-LCC, LCC-PBM, and PelB-LCC-PBM, were constructed with codon optimization and expressed in *E. coli* BL21(DE3) under the inducible T7 expression system, which aimed to improve the overall enzyme production in bioreactors, the binding efficiency of the produced enzyme on PET surface, and/or the enzyme's catalytic activities.

*E. coli* cells, like other Gram-negative bacteria, possess an inner and outer membrane that separates the organism into two main subcellular compartments: the cytoplasm and the periplasm. The most common choice to produce recombinant proteins is in the cytoplasm. However, the periplasmic space or the extracellular environment is more suitable when disulfide bonds are required for correct protein folding [40, 41], especially toxic heterologous recombinant proteins. In fact, the toxicity caused by the expression and accumulation of intracellular LCC led to decline of cell density after the *E. coli* reached its maximum DCWs within 20 h (**Figure S3 a**). LCC contains one disulfide bond, which contributes not only to the thermodynamic stability but also to the kinetic stability of LCC [42]. The disulfide bridge cannot be efficiently formed in the reducing condition of the cytoplasm [40]. To overcome the limitation of *E. coli* cytoplasm expression, we engineered the LCC with a signal sequence that directs them to the more oxidizing bacterial periplasm for proper folding. With the assistance of the N-terminal PelB leader sequence [31], about 30% of the recombinant PelB-LCC or PelB-LCC-PBM produced by *E. coli* was secreted to the culture medium **(Figure 1 a-d)**. The secretion of recombinant proteins not only facilitates downstream recovery but also offers other potential advantages. The translocation increases the cell viability (reduces cell toxicity) and enzyme yields, which is consistent with our results that the *E. coli* transformed with pPelB-LCC-PBM or pPelB-LCC plasmids showed higher cell densities (PelB-LCC > LCC and PelB-LCC-PBM > LCC-PBM) (**Figure S3 a**) and enzyme titers (PelB-LCC > LCC > PelB-LCC-PBM > LCC-PBM) **(Figure 1 a-d)**. In addition, the translocation also reduces the exposure of the recombinant enzyme to the cytoplasmic protease, thus reduces the enzyme degradation. Although the PelB signal peptide may be cleaved when it passes the inner periplasmic membrane, we found that the PelB-LCC purified from both cell pellets (intracellular) and fermentation supernatant (extracellular) had almost the same activity and both showed > 20% improvements over LCC. This suggests the produced PelB-LCC is most likely a mature protein.

Though it is believed that the PelB signal peptide can be cleaved by the signal peptidase during the translocation across the inner periplasmic membrane, resulting in the release of the mature protein into the periplasm, a few research studies indicated that the signal peptide may not necessarily be cleaved, or at least not completely cleaved from the linked protein [43-45]. In this study, the SDS-Page denaturing gels of the purified intracellular PelB-LCC (31.4 kDa) and LCC (28.8 kDa) showed that the former indeed had a higher molecular weight (**Figure 1e** and **Figure S7**), which suggests that the majority of the intracellular PelB-LCC stayed as a mature protein,

similar to what was observed by Deb A et al [45] using mass spectrometry and denaturing gels. However, it was also observed that the extracellular PelB-LCC showed a reduced molecular size, with a molecular weight very similar to LCC (**Figure S7**). It seemed that the PelB signal peptide was likely cleaved when the produced PelB-LCC was secreted into the extracellular medium. In the *E. coli* fermentation, about 70% of the PelB-LCC was produced intracellularly, which may have helped retain the PelB signal peptide [46, 47]. Interestingly, we observed that both extracellular and intracellular PelB-LCC showed very comparable PET biodegradation activity, which were both significantly higher than what was observed for the intracellular LCC. This suggested that the PelB signal peptide may not necessarily have a direct impact on LCC's catalytic activity. Instead, it was reported that the PelB signal peptide could influence the soluble protein levels and improve the bioactivity of protein owing to the slow aggregation process and shifting of the target protein to a folding pathway [48]. The cytoplasmic reducing conditions may contribute to the LCC misfolding and inclusion body formation. However, the desirable high level of protein expressions in industrial applications may lead to the aggregation and misfolding of desired proteins and resultantly affecting the function of protein. This negative effect on the activity of cutinase, has been experimentally observed in various studies [49, 50]. If the target protein is expressed in the cytosol with aggregation and misfolding, it generally lacks to fulfill its biological function [51]. With the help of secreting some of the produced enzyme to the extracellular medium, PelB-LCC exhibited higher catalytic activities on PET degradation as compared to other three $LCC^{ICCG}$ variants (**Figure 3 b** and **Figure 4 d**).

Apart from the active site area, the surface interaction of the cutinases and substrates appears to have a major impact on the hydrolysis of PET [32, 52]. If a PET hydrolase harbors a substrate-binding module linked via spacers to its catalytic domain, it may facilitate the adsorption of the enzyme during the natural hydrolysis of a polymer [27]. Enzymes with substrate binding domains have been shown not only to increase the amount of active enzyme on the polymer interface [53], but also to enhance the hydrolysis of insoluble substrates by partially disrupting the structure of the polymer and therefore making the targeted bonds more accessible to the catalytic domain [54-56]. To increase the adsorption of active enzymes on the PET interface, LCC enzymes were engineered to fuse a polymer-binding module (PBM) from *A. faecalis* via a linker from *T. reesei* to the C-terminus in this study. The PBM binding module has a hydrophobic nature that can help bind the enzyme on the hydrophobic surface of PET. Our results showed that adsorption to PET

by the LCC-PBM and PelB-LCC-PBM enzymes was almost doubled as compared with LCC and PelB-LCC **(Figure 3 a)**. Although the performance of PET hydrolysis of all four $LCC^{ICCG}$ constructions was much higher than that of the bacterial enzyme PETase from *Ideonella sakaiensis* 201-F6, the degradation efficiencies of LCC-PBM and PelB-LCC-PBM were not as high as LCC and PelB-LCC (**Figure 5** and **Figure 6**). The increased binding efficiency of PBM failed to improve PET degradation, which may be attributed to the complexity of the binding process and the formation of the active enzyme-substrate complex. Our unpublished data showed that the crystallinities of PET in aqueous solution gradually increased from 12% to ~30% in the first three days. Previous studies have shown that PET hydrolases preferably degrade the amorphous regions of PET [57-61], which is similar to what we observed in the biodegradation of low-crystallinity PET, where nearly 100% degradation rate was achied when the amorphas PET was employed as feedstock for the PelB-LCC reaction (**Figure 5 a-d**). Increased crystallinity limits the movement of the polymer chains and therefore, decreases the availability of polymer chains for enzymatic attack [62]. On one hand, enzyme should be bound to low-crystallinity (e.g., < 20%) PET surface to start the depolymerization process. On the other hand, if the enzyme happens to be bound to the high-crystallinity (e.g. > 30%) substrate, then it may no longer become available for a new enzymatic reaction, thereby limiting the overall depolymerization activity.

Biodegradation is a complex process and is governed by many factors, such as the availability of the substrate, surface topology, morphology, molecular weight of the polymer, and orientation of the polymer chains [62-65]. The accessibility of the polymer structure to enzymes and water depends primarily on crystallinity, hydrophobicity, and the steric effects of the side groups in the polymer backbone [66]. Different levels of PET degradability were shown in this study, especially based on the particle size of PET (i.e., specific surface area) and the degree of crystallinity. To improve biodegradation efficiency, recycled PET (RPET) was ground into smaller pellets to decrease particle size and increase the surface area. As a result, the degradation rate of LCC in the presence of smaller RPET particle sizes (with 60 mesh screen) was significantly improved **(Figure 4 b and d)**.

Genetic engineering methods can be used to create recombinant enzymes and/or microbial strains as the preferred strategy to enhance the biodegradation of synthetic petroleum-based plastic waste. Recently, advances in artificial intelligence and its application in protein design and engineering bring in new opportunities for discovering or creating new enzymes with significantly

higher catalytic activities. For example, Alper's group has used a machine learning algorithm to engineer *Is*PETase. The mutant enzyme, FAST-PETase, has an increased thermotolerance up to 50 ºC and demonstrated nearly complete degradation of some postconsumer PET within a week [20].

Small size reactions in tubes or shake flasks were efficient for screening enzymes and optimizing basic reaction conditions such as the temperature and initial PH values, but it is not necessary that these preliminarily determined conditions can be easily extended to large-scale applications. For example, using a phosphate buffer is enough to maintain the pH value within 7~8 in tube reactions with ~ 5 g/L PET substrate, but in a reactor with high-capacity PET loading, such as 200 g/L in the 1-L reactor study, concentrated base (KOH, NaOH) has to be continuously fed into the reactor to control the pH value and maintain the enzyme's activity. Other challenges including the inefficient mixing and mass transfer due to the use of high loadings of solid substrate (PET) and accumulation of insoluble product (TPA) may also become limiting factors in PET degradation. Therefore, scale-up experiments in reactors with high-capacity substrate loading is crucial for understanding the practical applications of the selected enzyme(s) and the optimized process conditions at large scale. More importantly, the scale-up experiments will provide key technical data for techno-economic analysis and identify the major limiting factors or technical barriers that may affect the commercialization opportunities. In this study, the top two $LCC^{ICCG}$ variants (namely LCC and PelB-LCC) were selected for further testing in a 1-L stirred tank bioreactor, which contained 200 g/L recycled PET. PelB-LCC improved PET degradation rate by > 20% over the original $LCC^{ICCG}$, which would lead to the reduction of either the use of the enzyme or the reaction time in a real application. In either case, this improvement suggests lower process cost, as analyzed by the earlier TEA study [34].

In the scaled-up experiments, crystallinity increase in substrate (PET) and enzyme instability may be the two major reasons that accounted for the gradual slow-down depolymerization rate after the first two or three days (**Figure 6 c-f**). The whitish color and the change to the opaque appearance of the undegraded PET material (**Figure 6 b**) suggested that the crystallinity of the surface of recycled PET have increased during the reaction, which was verified by DSC analysis as the crystallinity increased from 12% for the original material to ~ 30% for the undegraded PET materials after 72 h. This may have led to significantly less efficient degradation of PET since our previous research indicated that high crystallinity is one of the major challenges for efficient PET

degradation [22, 37]. Our preliminary research on the enzyme stability also indicated that the specific activities of LCC and PelB-LCC at 65 ºC may decline by 30% within 120 hours (**Figure S6**). The combined effects from both the crystallinity increase of PET and the enzyme instability may have led to the near stop of the PET depolymerization after 72 hours. Further research should be conducted to understand the enzymatic reaction mechanism at a large scale so that the limiting factors can be revealed, and the major barriers can be overcome. The continuing research may include improving the enzyme activity and stability, increasing the specific surface area of PET, and lowering the crystallinity by pretreating PET so that complete and fast degradation of post-consumer PET waste can be achieved.

## Conclusion

Enzymatic degradation provides an attractive approach for the biodegradation and biorecycling of post-consumer plastic wastes. The $LCC^{ICCG}$ showed significantly higher PET degradation efficiency than PETase (W159H/S238F) from *Ideonella sakaiensis* 201-F6 due to its higher thermostability and peak activity at 65 ºC. Four designed $LCC^{ICCG}$ variants including LCC, PelB-LCC, LCC-PBM, and PelB-LCC-PBM were expressed by the *E. coli* BL21(DE3). A fed-batch fermentation process was developed to produce the LCC enzymes up to 1.2 g/L within 36 hours. The PBM binding module doubled the binding efficiency of LCC on PET samples but failed to improve the degradation rate. The PelB unit not only helped secrete the produced enzyme but also improved PET degradation. In general, PET samples with smaller particle sizes and lower crystallinity had significantly higher degradation efficiency. Nearly complete degradation was achieved in tube reactions for amorphous PET films and extruded recycled PET particles treated with 0.2 μmol PelB-LCC/g PET for 72 hours. The developed enzymatic degradation process was scaled up in 1-L bioreactor experiments containing 200 g/L recycled PET pellets and 2 μM (or 60 mg/L) LCC or PelB-LCC, which demonstrated more than 80% degradation within three days. Further studies on enzyme engineering and stability, the enzymatic reaction mechanism, and the pretreatment of post-consumer waste PET materials are needed in future to achieve fast and complete degradation at a large scale.

## Acknowledgments

This work is supported by the Department of Energy (Award number EE0008930). The authors would also like to thank Dr. Gregg Beckham's research group at NREL for technical guidance and support during the research.

## Author Contributions

Ya-Hue Soong designed the experiments, analyzed the experimental data, and wrote the manuscript. Umer Abid performed the 1-L enzyme reaction experiments and helped write the manuscript. Allen C. Chang and Akanksha Patel helped prepare the recycled PET for experiments. Allen C. Chang also helped review and edited the manuscript. Christian Ayafor provided the HPLC analysis for all enzymatic reaction samples. Jin Xu helped conduct the protein gel analysis. Carl Lawton provided the general guidance in experiments of cell culture, molecular biology, and protein gel analysis. Hsi-Wu Wong and Margaret J Sobkowicz helped supervise the project, reviewed and edited the manuscript. Dongming Xie designed the project, provided technical guidance and supervision, and helped write the manuscript.

## Conflict of Interest

The authors declare no conflict of interest.

## Data Availability Statement

The research data from this paper are available from the corresponding author upon reasonable request.

# References


[1] PlasticSoupFoundation, *The world's population consumes 1 million plastic bottles every minute* 2017, pp. https://www.plasticsoupfoundation.org/en/2017/2007/the-worlds-population-consumes-2011-million-plastic-bottles-every-minute/.

[2] Coghlan, A., *Bacteria found to eat PET plastics could help do the recycling | New Scientist*, New Scientist 2016, pp. https://www.newscientist.com/article/2080279-bacteria-found-to-eat-pet-plastics-could-help-do-the-recycling/.

[3] Zhao, S., Wang, T., Zhu, L., Xu, P.*, et al.*, Analysis of suspended microplastics in the Changjiang Estuary: Implications for riverine plastic load to the ocean. *Water Research* 2019, *161*, 560-569.

[4] Narancic, T., O'Connor, K. E., Plastic waste as a global challenge: are biodegradable plastics the answer to the plastic waste problem? *Microbiology (Reading, England)* 2018, *165*, 129-137.

[5] Wei, R., Von Haugwitz, G., Pfaff, L., Mican, J.*, et al.*, Mechanism-Based Design of Efficient PET Hydrolases. *ACS Catalysis* 2022, *12*, 3382-3396.

[6] Carniel, A., Waldow, V. d. A., Castro, A. M. d., A comprehensive and critical review on key elements to implement enzymatic PET depolymerization for recycling purposes. *Biotechnology Advances* 2021, *52*, 107811-107811.

[7] Soong, Y.-H. V., Sobkowicz, M. J., Xie, D., Recent Advances in Biological Recycling of Polyethylene Terephthalate (PET) Plastic Wastes. *Bioengineering* 2022, *9*, 98.

[8] Müller, R. J., Schrader, H., Profe, J., Dresler, K., Deckwer, W. D., Enzymatic Degradation of Poly(ethylene terephthalate): Rapid Hydrolyse using a Hydrolase from T. fusca. *undefined* 2005, *26*, 1400-1405.

[9] Tanasupawat, S., Takehana, T., Yoshida, S., Hiraga, K., Oda, K., Ideonella sakaiensis sp. nov., isolated from a microbial consortium that degrades poly(ethylene terephthalate). *International Journal of Systematic and Evolutionary Microbiology* 2016, *66*, 2813-2818.

[10] Yoshida, S., Hiraga, K., Takehana, T., Taniguchi, I.*, et al.*, A bacterium that degrades and assimilates poly(ethylene terephthalate). *Science* 2016, *351*, 1196-1199.

[11] Egmond, M. R., De Vlieg, J., Fusarium solani pisi cutinase. *Biochimie* 2000, *82*, 1015-1021.

[12] Cunha, M. T., Costa, M. J. L., Calado, C. R. C., Fonseca, L. P.*, et al.*, Integration of production and aqueous two-phase systems extraction of extracellular Fusarium solani pisi cutinase fusion proteins. *Journal of Biotechnology* 2003, *100*, 55-64.

[13] Longhi, S., Cambillau, C., Structure-activity of cutinase, a small lipolytic enzyme. *Biochimica et biophysica acta* 1999, *1441*, 185-196.

[14] Ronkvist, Å. M., Xie, W., Lu, W., Gross, R. A., Cutinase-Catalyzed hydrolysis of poly(ethylene terephthalate). *Macromolecules* 2009, *42*, 5128-5138.

[15] Garza, D. R., Dutilh, B. E., From cultured to uncultured genome sequences: metagenomics and modeling microbial ecosystems. *Cellular and molecular life sciences : CMLS* 2015, *72*, 4287-4308.

[16] Parages, M. L., Gutiérrez-Barranquero, J. A., Reen, F. J., Dobson, A. D. W., O'Gara, F., Integrated (Meta) Genomic and Synthetic Biology Approaches to Develop New Biocatalysts. *Marine drugs* 2016, *14*.

[17] Sulaiman, S., Yamato, S., Kanaya, E., Kim, J. J.*, et al.*, Isolation of a Novel Cutinase Homolog with Polyethylene Terephthalate-Degrading Activity from Leaf-Branch Compost by Using a Metagenomic Approach. *Applied and Environmental Microbiology* 2012, *78*, 1556-1556.

[18] Kawai, F., Kawabata, T., Oda, M., Current State and Perspectives Related to the Polyethylene Terephthalate Hydrolases Available for Biorecycling. *ACS Sustainable Chemistry and Engineering* 2020, *8*, 8894-8908.

[19] Knott, B. C., Erickson, E., Allen, M. D., Gado, J. E.*, et al.*, Characterization and engineering of a two-enzyme system for plastics depolymerization. *Proceedings of the National Academy of Sciences of the United States of America* 2020, *117*, 25476-25485.

[20] Lu, H., Diaz, D. J., Czarnecki, N. J., Zhu, C.*, et al.*, Machine learning-aided engineering of hydrolases for PET depolymerization. *Nature 2022 604:7907* 2022, *604*, 662-667.

[21] Maity, W., Maity, S., Bera, S., Roy, A., Emerging Roles of PETase and MHETase in the Biodegradation of Plastic Wastes. *Applied Biochemistry and Biotechnology* 2021, *193*, 1-18.

[22] Tournier, V., Topham, C. M., Gilles, A., David, B.*, et al.*, An engineered PET depolymerase to break down and recycle plastic bottles. *Nature* 2020, *580*, 216-219.

[23] Brott, S., Pfaff, L., Schuricht, J., Schwarz, J. N.*, et al.*, Engineering and evaluation of thermostable IsPETase variants for PET degradation. *Engineering in Life Sciences* 2022, *22*, 192-203.

[24] Cui, Y., Chen, Y., Liu, X., Dong, S.*, et al.*, Computational Redesign of a PETase for Plastic Biodegradation under Ambient Condition by the GRAPE Strategy. *ACS Catalysis* 2021, *11*, 1340-1350.

[25] Graham, R., Erickson, E., Brizendine, R. K., Salvachúa, D.*, et al.*, The role of binding modules in enzymatic poly(ethylene terephthalate) hydrolysis at high-solids loadings. *Chem Catalysis* 2022, *2*, 2644-2657.

[26] Xue, R., Chen, Y., Rong, H., Wei, R.*, et al.*, Fusion of Chitin-Binding Domain From Chitinolyticbacter meiyuanensis SYBC-H1 to the Leaf-Branch Compost Cutinase for Enhanced PET Hydrolysis. *Frontiers in Bioengineering and Biotechnology* 2021, *9*, 1315-1315.

[27] Boraston, A. B., Bolam, D. N., Gilbert, H. J., Davies, G. J., Carbohydrate-binding modules: fine-tuning polysaccharide recognition. *Biochemical Journal* 2004, *382*, 769-769.

[28] Austin, H. P., Allen, M. D., Donohoe, B. S., Rorrer, N. A.*, et al.*, Characterization and engineering of a plastic-degrading aromatic polyesterase. *Proceedings of the National Academy of Sciences of the United States of America* 2018, *115*, E4350-E4357.

[29] Sambrook, J., Fritsch, E. F., Maniatis, T., Molecular cloning: a laboratory manual. *Molecular cloning: a laboratory manual.* 1989.

[30] Patel, A., Chang, A. C., Perry, S., Soong, Y.-H. V.*, et al.*, Melt Processing Pretreatment Effects on Enzymatic Depolymerization of Poly(ethylene terephthalate). *ACS Sustainable Chemistry & Engineering* 2022.

[31] Shi, L., Liu, H., Gao, S., Weng, Y., Zhu, L., Enhanced Extracellular Production of IsPETase in Escherichia coli via Engineering of the pelB Signal Peptide. *Journal of Agricultural and Food Chemistry* 2021, *69*, 2245-2252.

[32] Ribitsch, D., Yebra, A. O., Zitzenbacher, S., Wu, J.*, et al.*, Fusion of binding domains to Thermobifida cellulosilytica cutinase to tune sorption characteristics and enhancing PET hydrolysis. *Biomacromolecules* 2013, *14*, 1769-1776.

[33] Gamerith, C., Herrero Acero, E., Pellis, A., Ortner, A.*, et al.*, Improving enzymatic polyurethane hydrolysis by tuning enzyme sorption. *Polymer degradation and stability* 2016, *132*, 69-77.

[34] Singh, A., Rorrer, N. A., Nicholson, S. R., Erickson, E.*, et al.*, Techno-economic, life-cycle, and socioeconomic impact analysis of enzymatic recycling of poly(ethylene terephthalate). *Joule* 2021, *5*, 2479-2503.

[35] Brizendine, R. K., Erickson, E., Haugen, S. J., Ramirez, K. J.*, et al.*, Particle Size Reduction of Poly(ethylene terephthalate) Increases the Rate of Enzymatic Depolymerization But Does Not Increase the Overall Conversion Extent. *ACS Sustainable Chemistry & Engineering* 2022, *10*, 9131-9140.

[36] Pasula, R. R., Lim, S., Ghadessy, F. J., Sana, B., The influences of substrates' physical properties on enzymatic PET hydrolysis: Implications for PET hydrolase engineering. *Engineering Biology* 2022, *6*, 17-22.

[37] Chang, A. C., Patel, A., Perry, S., Soong, Y. V.*, et al.*, Understanding Consequences and Tradeoffs of Melt Processing as a Pretreatment for Enzymatic Depolymerization of Poly(ethylene terephthalate). *Macromolecular rapid communications* 2022, *43*.

[38] Jog, J. P., Crystallization of Polyethyleneterephthalate. *Journal of Macromolecular Science, Part C* 1995, *35*, 531-553.

[39] Bell, E. L., Smithson, R., Kilbride, S., Foster, J.*, et al.*, Directed evolution of an efficient and thermostable PET depolymerase. *Nature Catalysis 2022 5:8* 2022, *5*, 673-681.

[40] Sandomenico, A., Sivaccumar, J. P., Ruvo, M., Evolution of Escherichia coli Expression System in Producing Antibody Recombinant Fragments. *International Journal of Molecular Sciences* 2020, *21*, 1-39.

[41] Bhatwa, A., Wang, W., Hassan, Y. I., Abraham, N.*, et al.*, Challenges Associated With the Formation of Recombinant Protein Inclusion Bodies in Escherichia coli and Strategies to Address Them for Industrial Applications. *Frontiers in Bioengineering and Biotechnology* 2021, *9*.

[42] Sulaiman, S., You, D. J., Kanaya, E., Koga, Y., Kanaya, S., Crystal structure and thermodynamic and kinetic stability of metagenome-derived LC-cutinase. *Biochemistry* 2014, *53*, 1858-1869.

[43] Harrington, J. M., Nishanova, T., Pena, S. R., Hess, M.*, et al.*, A retained secretory signal peptide mediates high density lipoprotein (HDL) assembly and function of haptoglobin-related protein. *J Biol Chem* 2014, *289*, 24811-24820.

[44] de Souza, G. A., Leversen, N. A., Målen, H., Wiker, H. G., Bacterial proteins with cleaved or uncleaved signal peptides of the general secretory pathway. *Journal of Proteomics* 2011, *75*, 502-510.

[45] Deb, A., Johnson, W. A., Kline, A. P., Scott, B. J.*, et al.*, Bacterial expression, correct membrane targeting and functional folding of the HIV-1 membrane protein Vpu using a periplasmic signal peptide. *PLOS ONE* 2017, *12*, e0172529.

[46] Ng, D. T. W., Sarkar, C. A., Engineering Signal Peptides for Enhanced Protein Secretion from Lactococcus lactis. *Applied and Environmental Microbiology* 2013, *79*, 347-356.

[47] Köchl, R., Alken, M., Rutz, C., Krause, G.*, et al.*, The signal peptide of the G protein-coupled human endothelin B receptor is necessary for translocation of the N-terminal tail across the endoplasmic reticulum membrane. *J Biol Chem* 2002, *277*, 16131-16138.

[48] Chen, W., Wu, J., Chen, W., Hu, P., Wang, X., An approach to achieve highly soluble bioactive ScFv antibody against staphylococcal enterotoxin A in E.coli with pelB leader. *IOP Conference Series: Earth and Environmental Science* 2020, *512*, 012077.

[49] Caspers, M., Brockmeier, U., Degering, C., Eggert, T., Freudl, R., Improvement of Sec-dependent secretion of a heterologous model protein in Bacillus subtilis by saturation mutagenesis of the N-domain of the AmyE signal peptide. *Applied Microbiology and Biotechnology* 2010, *86*, 1877-1885.

[50] Gasser, B., Saloheimo, M., Rinas, U., Dragosits, M.*, et al.*, Protein folding and conformational stress in microbial cells producing recombinant proteins: a host comparative overview. *Microbial Cell Factories* 2008, *7*, 11.

[51] Vabulas, R. M., Raychaudhuri, S., Hayer-Hartl, M., Hartl, F. U., Protein folding in the cytoplasm and the heat shock response. *Cold Spring Harb Perspect Biol* 2010, *2*, a004390.

[52] Herrero Acero, E., Ribitsch, D., Steinkellner, G., Gruber, K.*, et al.*, Enzymatic surface hydrolysis of PET: Effect of structural diversity on kinetic properties of cutinases from Thermobifida. *Macromolecules* 2011, *44*, 4632-4640.

[53] Bolam, D. N., Ciruela, A., McQueen-Mason, S., Simpson, P.*, et al.*, Pseudomonas cellulose-binding domains mediate their effects by increasing enzyme substrate proximity. *The Biochemical journal* 1998, *331 ( Pt 3)*, 775-781.

[54] Din, N., Damude, H. G., Gilkes, N. R., Miller, R. C.*, et al.*, C1-Cx revisited: intramolecular synergism in a cellulase. *Proceedings of the National Academy of Sciences of the United States of America* 1994, *91*, 11383-11383.

[55] Murase, T., Suzuki, Y., Doi, Y., Iwata, T., Nonhydrolytic fragmentation of a poly[(R)-3-hydroxybutyrate] single crystal revealed by use of a mutant of polyhydroxybutyrate depolymerase. *Biomacromolecules* 2002, *3*, 312-317.

[56] Din, N., Gilkes, N. R., Tekant, B., Miller, R. C.*, et al.*, Non–Hydrolytic disruption of cellulose fibres by the binding domain of a bacterial cellulase. *Bio/Technology* 1991, *9*, 1096-1099.

[57] Gamerith, C., Zartl, B., Pellis, A., Guillamot, F.*, et al.*, Enzymatic recovery of polyester building blocks from polymer blends. *Process Biochemistry* 2017, *59*, 58-64.

[58] Donelli, I., Freddi, G., Nierstrasz, V. A., Taddei, P., Surface structure and properties of poly-(ethylene terephthalate) hydrolyzed by alkali and cutinase. *Polymer Degradation and Stability* 2010, *95*, 1542-1550.

[59] Welzel, K., Müller, R. J., Deckwer, W. D., Enzymatischer Abbau von Polyester-Nanopartikeln. *Chemie Ingenieur Technik - CHEM-ING-TECH* 2002, *74*, 1496-1500.

[60] Brueckner, T., Eberl, A., Heumann, S., Rabe, M., Guebitz, G. M., Enzymatic and chemical hydrolysis of poly(ethylene terephthalate) fabrics. *Journal of Polymer Science Part A: Polymer Chemistry* 2008, *46*, 6435-6443.

[61] Carr, C. M., Clarke, D. J., Dobson, A. D. W., Microbial Polyethylene Terephthalate Hydrolases: Current and Future Perspectives. *Frontiers in Microbiology* 2020, *11*, 2825-2825.

[62] Mohanan, N., Montazer, Z., Sharma, P. K., Levin, D. B., Microbial and Enzymatic Degradation of Synthetic Plastics. *Frontiers in Microbiology* 2020, *11*, 2837-2837.

[63] Harrison, J. P., Boardman, C., O'Callaghan, K., Delort, A. M., Song, J., Biodegradability standards for carrier bags and plastic films in aquatic environments: a critical review. *Royal Society Open Science* 2018, *5*.

[64] Ammala, A., Bateman, S., Dean, K., Petinakis, E.*, et al.*, An overview of degradable and biodegradable polyolefins. *Progress in Polymer Science (Oxford)* 2011, *36*, 1015-1049.

[65] Albertsson, A. C., Andersson, S. O., Karlsson, S., The mechanism of biodegradation of polyethylene. *Polymer Degradation and Stability* 1987, *18*, 73-87.

[66] Zambrano, M. C., Pawlak, J. J., Venditti, R. A., Effects of Chemical and Morphological Structure on Biodegradability of Fibers, Fabrics, and Other Polymeric Materials. *BioResources* 2020, *15*, 9786-9833.